




# Cooperative Scheduling of Source-Load-Storage for Microgrids with Electric Springs

Jiulong Sun\*, Yanbo Che\*\*†, Xiao Guo\*\*\*

\*,\*\*,\*\*\*Department of Electrical Engineering, Tianjin University, Tianjin , China

(2021234034@tju.edu.cn, ybche@tju.edu.cn, 1042236895@qq.com)

†Corresponding Author; Yanbo Che, Postal address, Tel: +86 138 2067 2692, ybche@tju.edu.cn

Received: 08.06.2023 Accepted:12.07.2023

**Abstract-** Since in microgrid, distributed power sources are random and fluctuating, and loads and energy storage devices are complex, these characteristics make the microgrid scheduling problem exceptionally complex. In the process of microgrid dispatching, to reduce economic costs and improve voltage stability, we propose a coordinated planning model of microgrid source-load-storage with electric spring (ES). The ES is connected in series with non-critical loads to form smart loads, and through the use of smart loads, distributed power sources, loads and energy storage devices in the microgrid are simultaneously dispatched together. The objective function of the scheduling model is divided into two parts. The first part is the optimal economic cost, including the cost of charging and discharging energy storage, the cost of power purchase, the cost of wind and light abandonment, the cost of reliability and the additional cost corresponding to the introduction of ES; the second part is the optimal voltage balance of the microgrid, i.e., the minimum voltage deviation. In the process of model search, a model solving method considering load demand is proposed to quantitatively analyze the proposed energy optimization model and find the optimal scheduling scheme. Results show that the model can reduce the operating cost and optimize the voltage level of the distribution network under various scenarios, thus verifying the correctness and effectiveness of the proposed model.

**Keywords** Microgrid, electric spring, distributed generator, voltage stability, source-load-storage coordinated planning.

Nomenclature			
<b>Abbreviations</b>		PSO	particle swarm optimization algorithm
BESS	battery energy storage system	PV	photovoltaic
CL	critical load	WT	wind turbine
DG	distributed generator	<b>Sets</b>	
DLC	Direct Load Control	$l$	total number of controllable DGs
ES	electric spring	$W$	total number of scenarios with different new energy output
EXP	energy excess rate		
ES-BTB	electric spring Back-to-Back	$N$	total number of optimization intervals
IL	Interrup- tible Load	<b>Indices</b>	
LPSP	loss of power supply probability	$t$	time
NL	non-critical load	$\omega$	scenario

## 1. Introduction

With the rapid development of the global economy and the growing population, the supply of traditional energy

sources can no longer meet the needs of the people. renewable energy, as a new form of energy, has broad application prospects and important strategic significance.

Microgrid can effectively integrate renewable energy and traditional energy sources, which is an important platform for effective multi-point decentralized access of distributed generator (DG) and its effective utilization[1]. However, renewable energy is highly unstable, and when large-scale DG is connected to the microgrid, a series of problems such as voltage dips and frequency fluctuations are likely to arise, which makes microgrid scheduling more difficult. In order to solve these problems, the cooperative scheduling of source-load-storage of microgrid becomes the key to microgrid operation optimization.

Source-load-storage cooperative scheduling refers to the rational dispatching of various energy devices in microgrid according to load demand and energy supply to achieve the balance and optimal utilization of energy. The optimization problem of source-load-storage cooperative scheduling involves several factors, such as load prediction, energy supply, energy storage device control, etc [2].

In microgrid, loads with high power quality requirements are generally called critical loads (CL), which receive little regulation, such as medical equipment, monitoring and communication equipment involved in the security of the microgrid area. Loads that can operate in a wider voltage range are called non-critical loads (NL), which mainly include 2 categories: the first category is approximately purely resistive, with a power factor of about 0.99, such as electric heating loads and unimportant lighting; the second category is resistive loads, such as solid-storage electric furnaces with thermal efficiency of more than 95% and a power factor of about 0.8, which can work during low valley tariff hours or actively consume renewable energy and store thermal energy for use during other hours [3].

Various studies have been conducted for microgrid scheduling, which involve various aspects such as power, load, and energy storage. Reference [4] knot proposed a multi-objective scheduling model for hybrid microgrids, using elastic prices of load demand as a linear function to optimize the electricity price, thus maximizing the profit of the power company and the demand of the customers. Reference [5] introduced an economic scheduling strategy for microgrids with multiple energy storage systems, which realized the cooperative management of traditional energy storage methods and distributed energy storage in microgrids through a central controller of the microgrid, thus achieving the consumption of surplus energy and improving the economy. Reference [6] proposes a two-stage optimal energy dispatching strategy for microgrid clusters considering the economy and stability of the microgrid cluster system, so as to coordinate the economic benefits and operational risks of the microgrid, and uses an improved particle swarm optimization algorithm (PSO) to find out the optimal solution for the dispatching strategy, and reference [7] integrates a battery energy storage system (BESS) and a solar photovoltaic (PV) unit into a combined solar storage system, thus proposing a multi time scale, two-stage robust unit commitment and economic dispatching model to optimize microgrid operation. In summary, the current dispatching mainly adopts economic means or new technologies at the load and storage ends to reduce the microgrid system operation cost by a single

regulated power source or energy storage under the fixed load demand, but does not essentially optimize the microgrid for source-load-storage coordination, and the optimization goal focuses on economy, with less consideration on power quality, especially voltage stability.

Electric spring (ES) is a new type of power electronic equipment with voltage and power regulation capability, which can store electrical energy and provide voltage support for the grid and suppress voltage fluctuations.

By connecting in series with NLs or energy storage devices, ES can form intelligent loads and adaptively regulate the parallel CLs, thus achieving voltage stability and energy buffering [8]. In the field of distribution networks, ES research has focused on topologies and control strategies. Electric spring Back-to-Back (ES-BTB) are able to achieve coordinated control of both active and reactive power [9]. Reference [10] compares the topologies of ES and ES-BTB in distribution networks and finds that ES-BTB has better economics by eliminating the need to connect batteries in parallel on the DC side. Reference [11] introduced a an ES control strategy and working principle in an islanded microgrid to control the load and voltage balance of the hot water system by means of model scheduling control. Reference [12] proposed a two-stage ES-based voltage management scheme to maintain the grid voltage stability by coordinating two types of voltage regulating devices with different response rates together.

In summary, based on the above discussion, we can find that ES access can provide good voltage and power regulation for the microgrid and achieve coordinated source-load-storage optimization. However, there is a lack of sufficient research on the scheduling of ES in microgrid systems, especially on the coordinated scheduling of ES and other devices as well as their economical problems associated with ES participation in microgrid scheduling.

To bridge the gap, this paper attempts to establish a source-load-storage coordinated scheduling model, in which ES-B2B is used and we take into account the economics and voltage levels in the dispatching process, and performs multi-objective optimization of energy storage charging and discharging costs, wind and light abandonment costs, power purchase costs, ES equipment depreciation costs, load regulation subsidy costs, reliability costs and voltage deviation at each node of the microgrid, so as to achieve coordinated source-load-storage optimization and further to analyze the effect of ES on NLs and energy storage. It further analyzes the economic benefits and power quality assurance of ES for NLs and energy storage devices when they are connected to the microgrid with distributed power sources. For the selection of the optimal planning scheme, this paper solves the optimization model based on the load loss rate and energy surplus rate for the NLs. Finally, the ES-enabled source-load-storage scheduling scheme is analyzed under different scenarios of distributed power supply output, load power factor and tariff through simulation examples to verify the superiority of the scheme in terms of economic improvement and voltage level improvement.

**2. Microgrids and Electric Springs Topologies**

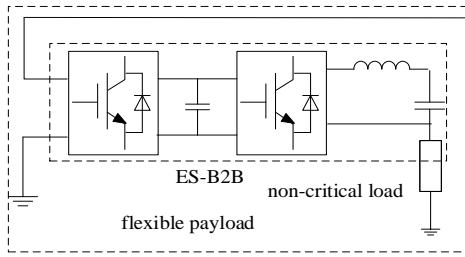


**Fig. 1.** ES-BTB topology.

Various types of topologies have been studied for electric springs, among which ES-BTB can achieve coordinated

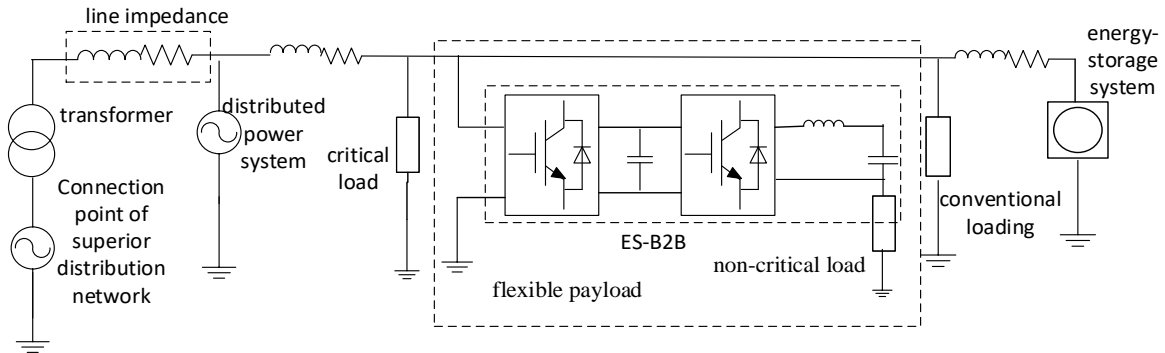


**Fig. 2.** Schematic diagram of microgrid with ES.

In microgrid with a high proportion of renewable energy, CLs still require high levels of reliability. However, sacrificing voltage quality for NLs is not a viable option. The extent to which NLs can be regulated depends on their own load characteristics as well as subsidies and customer willingness to participate. The minimum electricity consumption required for Intelligent loads is determined by both the customers' willingness to be regulated and the operational needs of the microgrid in which they are located.

The NL regulation means proposed by us are distinguished from existing adjustable loads [18-20], which include interruptible load (IL) and direct load control (DLC) loads. Intelligent loads have both upward and downward regulation spaces, and both interruptible loads and direct load control loads not be modelled in this paper can only respond to energy optimization objectives by reducing electricity consumption [21]. A portion of adjustable loads and NLs that are not continuously regulated can likewise receive continuous regulation by using ES as the regulating medium. Set  $V_s$  as the voltage of the intelligent load, the upper limit of active load regulation  $P_{max}$  of the intelligent load is calculated as follows:

$$P_{max} = \frac{V_s^2}{Z_{NL} \cos \varphi} \tag{1}$$

where  $\varphi$  is the power factor angle of the non-critical load, and  $Z_{NL}$  is the impedance size of the non-critical load.

control of both active and reactive power at a lower economic cost [13-14], and its topology is shown in Fig. 1.

One of the control loops is an ES control loop based on a proportional-integral controller, which uses a phase-locked loop to regulate the phase of the real-time current flowing through the ES and the ES voltage [15]. The control loop converts the DC voltage to the output voltage of the ES according to the upper level requirements. The ES voltage and current phase difference is  $0^\circ$  or  $180^\circ$  to control the active power of the ES [16].

The basic topology of a microgrid containing ES-BTB is shown in Fig.2. In this case, the ES is concatenated with NLs to form Intelligent loads, and then concatenated with CLs to form power consumption groups [17].

**3. Cooperative Dispatching Model of Microgrid Source-Load-Storage with Electric Springs**

The energy optimization model in this paper is applied to low-voltage microgrids with access to ES and is oriented to microgrid operators. The operator purchases power from the long-term bilateral market and the day-ahead spot market when the microgrid is short of its own power, and only considers the case where the microgrid load does not affect the day-ahead market tariff [23]. The microgrid power is partly purchased by the operator from the long-term market and the day-ahead market, and partly from the DG, which is assumed to be owned by the operator, and only the generation cost of the controllable DG is considered. In this paper, controllable DG is exemplified by gas turbine generators and uncontrollable DG is exemplified by wind turbine generators and photovoltaic generators.

*3.1. Objective Function Properties*

The loss of power supply probability (LPSP) and energy excess rate (EXP) are chosen to characterize the level of reliability of the system and the level of energy excess generated to achieve reliable operation; LPSP expects that the system can satisfy the power balance constraint at any time, The EXP and LPSP want the system to satisfy the power balance constraint at any time, and the EXP wants the power output from the distributed power source not to overflow, i.e., ideally no energy is wasted in the independent microgrid and the power balance constraint is satisfied at all times [24-26]. The calculation is given by:

$$\delta_{LPSP} = \frac{\sum_{t=1}^N P_{loss}(t)}{\sum_{t=1}^N P_{load}(t)} \quad (2)$$

$$\delta_{EX} = \frac{\sum_{t=1}^N P_{EX}(t)}{\sum_{t=1}^N P_{load}(t)} \quad (3)$$

Where  $\delta_{LPSP}$ ,  $\delta_{EX}$ ,  $P_{loss}(t)$ ,  $P_{EX}(t)$  and  $P_{load}(t)$  are the load power loss rate, energy excess rate and t-time power loss, excess power, and t-time load level, respectively[27].

### 3.2. Total Objective Function

As shown in Fig. 3, a multi-objective scheduling model for stand-alone scenic storage microgrid is established with the overall objective including maximizing the economic benefits and optimal voltage stability of each node of the microgrid, calculated as

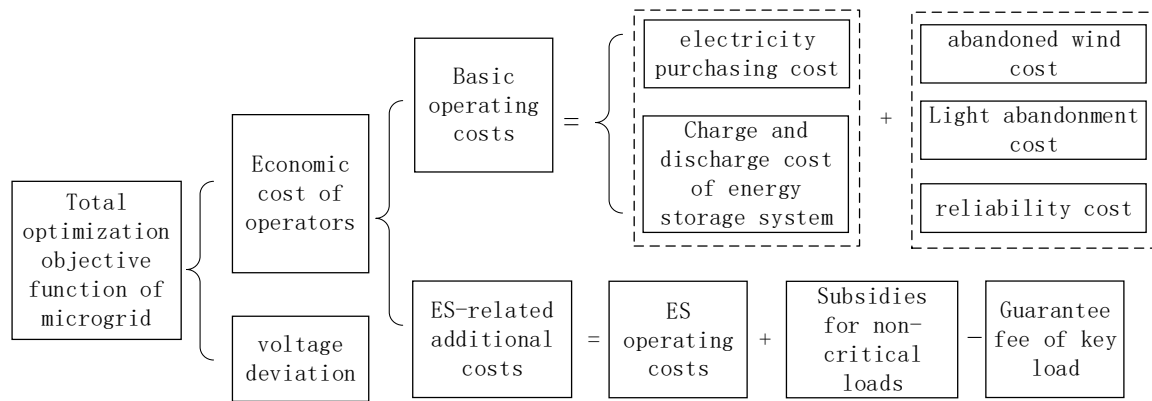


Fig. 3. Model objective function.

### 3.3. Economic Cost of Operators

The total economic cost for the microgrid operator  $C_F$  is calculated as

$$C_F = C_{FF} + C_{FS} \quad (6)$$

$$C_{FF} = F_1 + F_2 + F_3 + F_4 + F_5 + F_6 \quad (7)$$

$$C_{FS} = S_1 + S_2 - S_3 \quad (8)$$

where the base operating costs of the microgrid ( $C_{FF}$ ) mainly include the cost of purchasing electricity from the electricity market for the microgrid ( $F_1$ ), the operating cost of the controllable DG ( $F_2$ ), the cost of charging and discharging the energy storage system ( $F_3$ ), the cost of wind abandonment ( $F_4$ ), the cost of light abandonment ( $F_5$ ), and the cost of reliability ( $F_6$ ).  $C_{FS}$  The additional cost of introducing electric springs,  $S_1$  is the operating cost for ES, i.e., depreciation and maintenance of ES equipment;  $S_2$  is the subsidy cost to be paid by the microgrid operator for NLs, and  $S_3$  is the guarantee fee that is acceptable for CL customers to pay for a highly reliable power supply in addition to the normal power purchase cost [28]. The meaning and calculation of each component cost are as follows:

$$\min S = \lambda_1 C_F' + \lambda_2 \Delta U' \quad (4)$$

$$C_F' = \frac{C_F}{C_{F0}} \quad (5)$$

where  $C_F'$  is the normalized value of the total economic cost of the microgrid operator,  $\Delta U'$  is the normalized value of the voltage deviation during operation,  $\lambda_1$  and  $\lambda_2$  are the weight coefficients, and the weights can be set equal to ensure the economy and safety of operation.  $\lambda_1 = \lambda_2 = 0.5$ .  $C_F$  is the total economic cost of the microgrid operator,  $\Delta U$  is the average deviation of the nodes;  $C_{F0}$  is the lowest cost of the distribution network without considering ESs and distributed power sources, but the objective optimization solution.

(1) The cost of purchasing electricity from the electricity market for microgrid

$$F_1 = \sum_{t=1}^N [\lambda_t^{bmbuy} k_{bm} G_t + \lambda_t^{smbuy} (1 - k_{bm}) G_t] \Delta t \quad (9)$$

$$\Delta t = \frac{24}{N} \quad (10)$$

where  $F_1$  is the cost of electricity purchased by the microgrid from the electricity market;  $N$  is the total number of optimization intervals,  $\lambda_t^{bmbuy}$  and  $\lambda_t^{smbuy}$  are the prices of electricity purchased from the long-term bilateral market and the day-ahead spot market, respectively, at time  $t$ ;  $k_{bm}$  is the percentage of electricity purchased from the long-term market, which is the optimization variable, and the optimization result depends on the level of electricity prices in the day-ahead market;  $G_t$  is the total amount of electricity purchased through the long-term and day-ahead markets;  $\Delta t$  is the duration of the optimization interval.

(2) Operating cost of controllable DG

$$F_2 = \sum_{t=1}^N \left( \mu_D \sum_{i=1}^I D_{i,t} \right) \Delta t \quad (11)$$

where  $F_2$  is the operating cost of controllable DG;  $\mu_D$  is the unit price of generation of controllable DG;  $D_{i,t}$  is the output of the  $i$ -th controllable DG in the  $t$ th optimization interval;  $I$  is the total number of controllable DGs;

(3) Energy storage system charging and discharging costs

$$F_3 = \sum_{t=1}^N (k_{s,a} k_{s,i} + k_{s,m}) (S_{c,t} + K_{dc} S_{d,t}) \Delta t \quad (12)$$

$$k_{s,a} = \frac{r}{1 - (1+r)^{-N_s}} \quad (13)$$

Where  $k_{s,a}$  is the annuity factor converted from the initial value of energy storage investment to each year;  $k_{s,i}$  is the investment cost per unit of energy storage charging and discharging power;  $k_{s,m}$  is the operation and maintenance cost of energy storage;  $S_{c,t}$  and  $S_{d,t}$  are the charging and discharging power of energy storage battery respectively; the unit price of energy storage discharging cost is  $K_{dc}$  times of the unit price of charging cost, if the operator owns the energy storage, then the charging and discharging cost is generally the same, i.e.,  $K_{dc} = 1$ , if the operator leases the energy storage from the third party company, then The discharging cost is generally higher than the charging cost;  $r$  is the interest rate;  $N_{ES}$  is the life cycle of ES.

(4) Wind abandonment cost

$$F_4 = \sum_{t=1}^N \sigma_w (k_{wf} W_t^f - W_t) \Delta t \quad (14)$$

where  $\sigma_w$  is the wind abandonment penalty factor;  $W_t^f$  and  $W_t$  are the wind power forecast expectation and actual grid power respectively;  $k_{wf}$  is the wind power forecast accuracy,  $k_{wf} \geq 1$ , the higher the accuracy the closer the value is to 1;

(5) Cost of light abandonment

$$F_5 = \sum_{t=1}^N \sigma_{pv} (k_{w_{pv}} W_{tpv}^f - W_{tpv}) \Delta t \quad (15)$$

where  $\sigma_{pv}$  is the abandonment penalty factor;  $W_{tpv}^f$  and  $W_{tpv}$  are the wind power forecast expectation and actual grid power, respectively;  $k_{w_{pv}}$  is the wind power forecast accuracy,  $k_{w_{pv}} \geq 1$ , the higher the accuracy, the closer the value to 1;

(6) Reliability cost

For the two evaluation indicators, LPSP and EXR, they are factored into the objective function and described by the penalty function method, which is calculated as follows:

$$F_6 = \lambda_L \delta_{LPSP} + \lambda_E \delta_{EX} \quad (16)$$

where  $\lambda_L$  is the power loss penalty coefficient, set to  $10^5$  to ensure the reliability of the power supply;  $\lambda_E$  is the energy excess penalty coefficient, set to  $10^3$  to limit the large energy excess [29].

(7) Operating expenses of ES

$$S_1 = (k_{ES,a} k_{ES,i} + k_{ES,m}) |\Delta P_{k,t}^{ES}| \Delta t \quad (17)$$

$$k_{ES,a} = \frac{r}{1 - (1+r)^{-N_{ES}}} \quad (18)$$

where  $k_{ES,a}$  is the annuity factor converted from the initial value of ES investment to each year;  $k_{ES,i}$  is the investment cost corresponding to the reduction in electricity consumption per unit of smart load regulated by ES;  $k_{ES,m}$  is the operation and maintenance cost of ES;  $N_s$  is the life cycle of energy storage battery;  $r$  is the interest rate;  $N_{ES}$  is the life cycle of ES.

(8) Cost of subsidies to be paid for NLs

$$S_2 = \sum_{t=1}^N \left( \mu_{IL} \sum_{j=1}^J \Delta P_{j,t}^L + \mu_{ES} \sum_{k=1}^K |\Delta P_{k,t}^{ES} - \Delta P_{k,t}^{resp}| \right) \Delta t \quad (19)$$

where  $\mu_{IL}$  is the unit regulation compensation for interruptible loads;  $\mu_{ES}$  is the unit regulation allowance for smart loads;  $J$  is the number of interruptible loads;  $K$  is the number of smart loads;  $\Delta P_{j,t}^{IL}$  is the reduction of the  $j$ th interruptible load;  $\Delta P_{k,t}^{ES}$  is the reduction of the  $k$ th NL subject to ES regulation;  $\Delta P_{k,t}^{resq}$  is the amount of smart loads subject to ES regulation for the  $k$ th NL;

(9) Guarantee fee that CL users are willing to pay

CLs and NLs form a power consumption group. Some NLs are willing to sacrifice their own voltage quality in exchange for subsidy benefits so as to optimize their own power consumption costs, while CLs need to pay a guarantee fee for a highly reliable power supply in addition to the normal power purchase cost, which is calculated by the formula

$$H = \sum_{t=1}^N (P_{CL,t} \Delta \lambda_t) \Delta t \quad (20)$$

where  $P_{CL,t}$  is the CL volume for the  $t$  optimization interval;  $\Delta \lambda_t$  is the additional unit time guarantee cost that the CL is willing to subscribe to for the  $t$  interval.

3.5. Energy Optimization Model in Multiple Scenarios

In the above energy optimization model, maximizing economic efficiency is the optimization objective based on the determined distributed power output, load demand and day-ahead market time-of-use tariff. To enhance the applicability of the model to different operation scenarios, this paper integrates the uncertainties arising in the multi-scenario description microgrid model and takes the source-load-storage cooperative optimization objective function  $S_d$  under multiple scenarios as the optimization objective, as shown in equation (21).

$$\min S_{\omega} = \sum_{\omega=1}^W \pi_{\omega} S_{\omega}$$

(21)

where  $W$  is the total number of scenarios with different new energy output, load and day-ahead tariff;  $\pi_{\omega}$  is the probability of scenario  $\omega$ ;  $S_{\omega}$  is the total optimization objective function corresponding to scenario  $\omega$ . The specific value of  $\omega$  can be obtained by cluster analysis of the daily load curve, and the specific method of which can be found in the Reference [22]. The energy optimization model considering the uncertainty of source, load and day-ahead tariff is constructed based on the aforementioned deterministic energy optimization model using the multi-scenario description method, with the constraints of individual scenarios similar to those in Section 2.2, and the total number of constraints is  $W$  times that of individual scenarios[30].

#### 4. Model Solving Method

Based on the mathematical model of the scenery, the average hourly output of renewable energy is calculated as an input to find the amount of inequality that needs to be filled in order to meet the load demand for non-renewable energy sources as

$$P_{imb}(t) = N_{WT}P_{WT}(t) + N_{PV}P_{PV}(t) \tag{22}$$

In Eq. (22):  $P_{imb}(t)$  is not level, there are three possible cases at this point.

(1)  $P_{imb}(t) = 0$ , i.e., the power balance between renewable energy and load is satisfied at that moment, and there is no need to dispatch non-renewable energy, but since the scenery output is related to the environmental conditions, and the load is usually cyclical, such cases are almost non-existent.

(2)  $P_{imb}(t) > 0$ , that is, the renewable energy output exceeds the load demand at that moment, resulting in excess energy, the treatment has the following three steps: (1) priority scheduling of battery charging; (2) if there is still surplus energy, the intelligent load upward adjustment is invoked through the electric spring, which includes making the interruptible load work normally and making the levelable load adjust to other time periods; (3) if there is still surplus energy, the excess energy power is calculated, the formula is

$$P_{EX}(t) = P_{imb}(t) - S_{c,t} - P_{uve}(t) \tag{23}$$

where  $P_{uve}(t)$  is the output power of ES adjusted upward.

(3)  $P_{imb}(t) < 0$ , that is, the renewable energy output can not meet the load demand at that moment, there are some loads lose power, the processing has the following three steps: ① priority scheduling battery for discharge; ② if still can not meet the load demand, call the electric spring to call the intelligent load downward adjustment, which includes making the interruptible load interrupt work, making the other time panning load adjust to change the time to supplement; ③ if

the energy still has not enough, calculate the power loss, the formula is

$$P_{loss}(t) = |P_{imb}(t)| - S_{dt} - P_{dve}(t) \tag{24}$$

where  $P_{dve}(t)$  is the input power of ES adjusted downward. After obtaining the power loss and energy excess power, LPSP and EXR can be calculated according to Eq. (5) and Eq. (6).

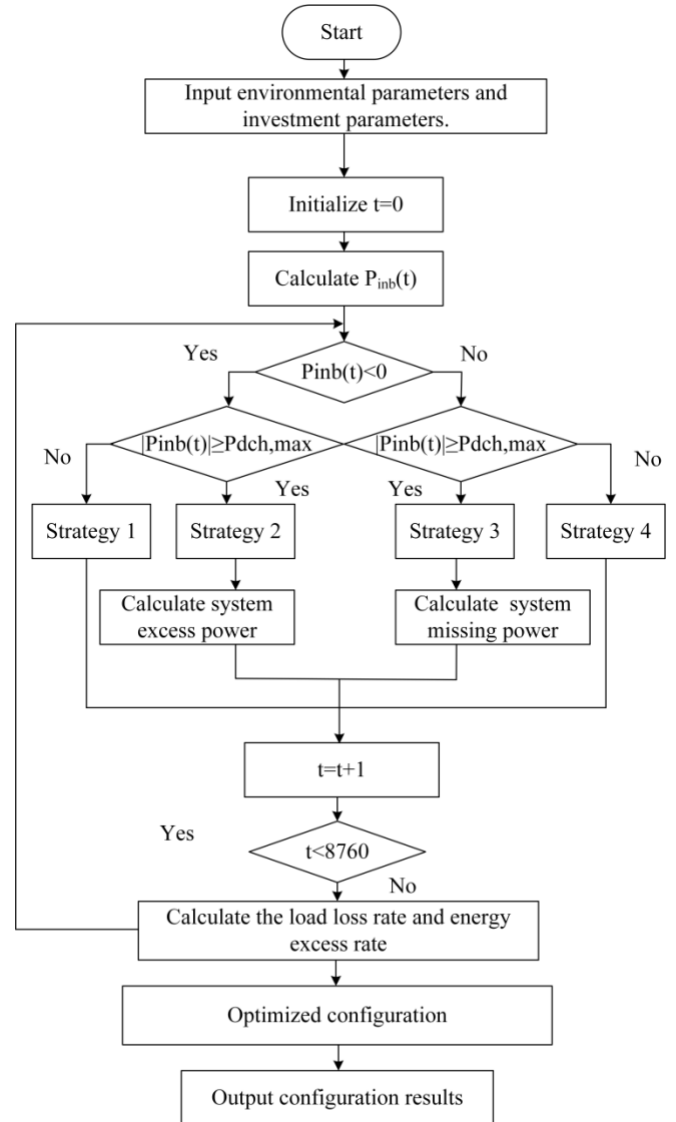


Fig. 4. Optimal power allocation process considering electric springs.

The specific solution method of the model is shown in Fig. 4. After inputting the parameters, different scenarios are distinguished according to the calculation of the inequality measure  $P_{imb}(t)$ , and the strategies corresponding to each scenario are as follows:

Strategy 1: after satisfying the power required by the load, the excess power of the power generation system charges the battery until it is full;

Strategy 2: after satisfying the power required by the load, the maximum charging power of the battery and the power of the electrolytic cell, the electric spring storage is started and

rushed to the maximum, and the excess power is calculated  $P_{EX}$ .

Strategy 3: When the new energy output is insufficient, the battery works to fill up the shortage of power;

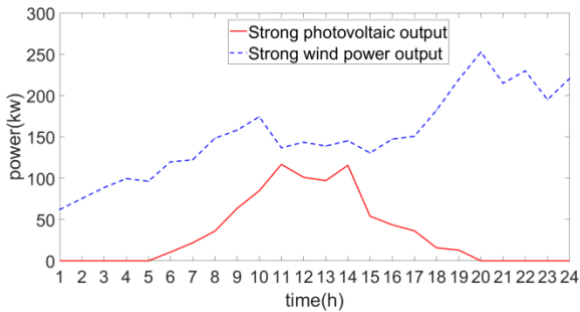
Strategy 4: When the new energy output is insufficient and the battery has reached the maximum discharge power, the electric spring starts to work and calculates the shortage of power  $P_{loss}$ .

**5. Analysis of Calculation Cases**

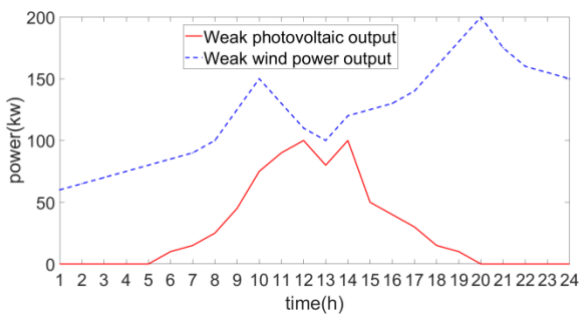
*5.1. Parameter Setting*

In order to verify the correctness of the proposed energy optimization model for microgrid containing ES in this paper, the above energy optimization model is developed in MATLAB2019n environment and the MATLAB-based YALMIP toolkit and CPLEX are used as solvers.

The microgrid consists of conventional thermal generating units (set as gas turbine units in this paper) power generation and distributed power generation together, conventional gas turbines maintain 65kW power in 24h of a day: since wind power and photovoltaic have instability in grid operation, two scenarios of strong wind power, photovoltaic power generation and weak wind power photovoltaic power generation are set respectively after investigating the law in a certain place in a year typical day, the corresponding wind and light output curve is shown in Fig. 5.



(a) Typical daily curve of weak wind power and photovoltaic power output



(b) Typical daily curve of strong wind power and photovoltaic power output

**Fig. 5.** Two typical daily curves of wind power and photovoltaic power output on typical days

The parameters of used microgrid, energy storage equipment and load are shown in Table A1、Table A2 and Table 3 in Appendix A, respectively.

The typical daily tariff curves are shown in Fig. 6, which are selected from the high day-ahead tariff and low day-ahead tariff for power exchange between the distribution network and the microgrid.

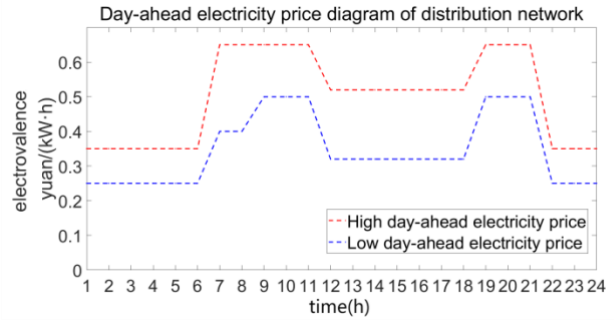


**Fig. 6.** Day-ahead electricity price diagram of distribution network.

By counting the total grid demand load, the total interruptible load, the total NL receiving ES regulation and the total CL in the microgrid arithmetic example, the inputs to the model are shown in Figure 7.

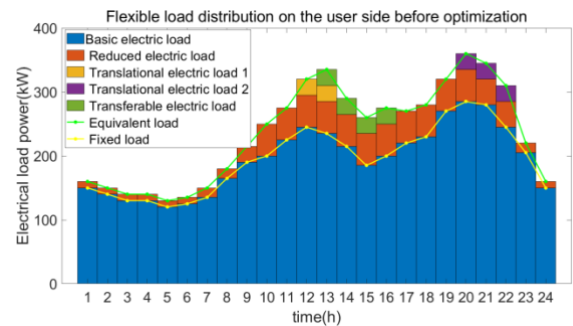


**Fig. 7.** Flexible load distribution on the user side before optimization.

*5.2. Energy Optimization Analysis of a Single Scene*

The scenario when the microgrid wind and PV power output is small, the day-ahead tariff is low, and the power factor of NLs is low is selected, and ES is used to regulate NLs. For the model proposed in this paper, the population size of the particle swarm algorithm is set to 40, the number of iterations is 150, the quantum particle swarm algorithm with improved chaotic mapping is used to find the optimal solution of the scheduling scheme, the load loss rate is set to 2% respectively, and the energy excess rate are set to 100%, and the optimization results after considering the electric spring are obtained using the model solving strategy in Fig. 4, and the load distribution after operation is shown in Fig. 8. The load distribution after operation is shown in Fig. 8.



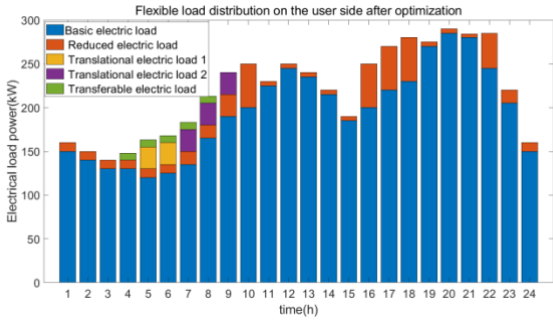


**Fig. 8.** Flexible load distribution on the user side after optimization.

Comparing the electric load curves before and after optimization, it can be seen that for each smart load, under the scheduling of ES participation, the levelable load 1 is leveled from 19:00~22:00 to 05:00~08:00, and the levelable load 2 is leveled from 11:00~13:00 to 15:00~17:00, and both levelable load 1 and levelable load 2 are leveled from the peak tariff hours to the relatively lower tariff Table 3 shows that the duration of the shiftable load remains unchanged and the power consumption during the shiftable load is the same as the original one, while the duration and power consumption of the shiftable load are changed, and the power distribution is more flexible compared with the shiftable load. In summary, the overall trend of shiftable and transferable flexible power loads from peak hours to valley and normal periods is conducive to the consumption of clean energy, and the shift of loads to valley and normal periods ensures the economy of dispatch. In addition, the load is subject to different degrees of curtailment, and the curtailment periods are mostly peak periods.

In this scenario, the electrical load of the microgrid is balanced during the day, and the individual energy output, battery charging and discharging, and the power purchase from the microgrid are shown in Fig. 9.

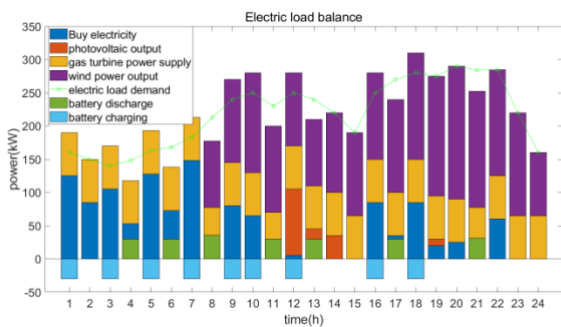
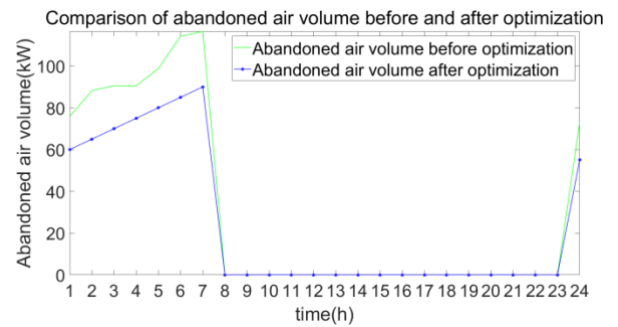


**Fig. 9.** Optimized power output of each energy source.

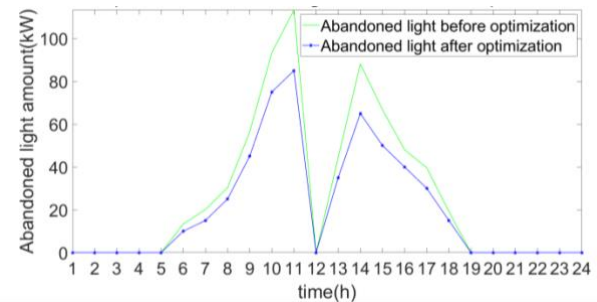
As shown in Fig. 9, the electric load is mainly met by the new energy and gas turbine output and the electric load balance of the microgrid is regulated by purchasing and selling electricity from the power market and battery charging and discharging, at the same time, the battery discharging relieves the pressure of power supply at peak hours. During the whole dispatching cycle, the gas turbine output plays a role in emission reduction on the one hand, and reduces the power impact on the grid during the scarcity of scenery resources and peak hours on the other. At the same time, ES also plays a

certain role of virtual energy storage by regulating NLs, which is reflected in the following ways: when wind power and photovoltaic power generation are rich, ES regulates NLs to increase active power consumption, which reduces storage charging power and promotes the consumption of new energy power generation; when wind power and photovoltaic power generation are poor, ES regulates NLs to reduce active power consumption, which reduces storage discharging power and fills the gap of new energy power generation. When wind power and photovoltaic power generation are poor, ES regulates NLs to reduce active power consumption, thus reducing energy storage discharge power and filling the gap of new energy generation.

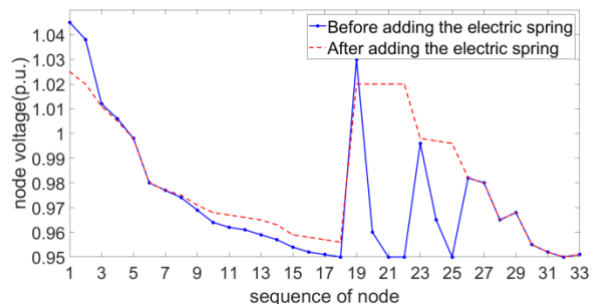
In order to verify the superiority of the proposed model, the wind abandonment, light abandonment, voltage deviation and each cost in 24h before and after optimization are compared, as shown in Fig. 10 and Table 2, respectively.



(a) Comparison of wind disposal volume before and after optimization



(b) Comparison of the amount of light abandoned before and after optimization





(c) Comparison of voltage deviation before and after optimization

**Fig. 10.** Comparison of results before and after optimization

**Table 1.** Cost comparison before and after optimization

	Before optimization (yuan)	After optimization (yuan)	Amount of change (yuan)
$C_F$	6313.51	6092.12	-221.39
$C_{FF}$	6313.51	6056.83	-256.68
$C_{Fs}$	0	35.29	35.29
$F_1$	2586.30	2553.50	-32.80
$F_2$	51.65	45.36	-6.28
$F_3$	574.85	509.39	-64.56
$F_4$	1118.72	1073.65	-45.07
$F_5$	1295.69	1271.37	-24.32
$F_6$	686.30	603.56	-82.74

As shown in Fig. 10, compared with the dispatching using only battery charging and discharging and distribution network purchase and sale, the amount of wind and light abandoned by the microgrid at different time periods is reduced to some extent by dispatching the curtailable and transferable loads, and after adding electric springs for regulation, ES further dissipates distributed energy and reduces the amount of wind and light abandoned by regulating the NLs. In addition, it can be seen from Figure 10c that the voltage of nodes 17, 18, 20 to 25, where the voltage is at a low level, are all improved to different degrees through the use of electric springs, and the voltage gap between adjacent nodes is reduced.

As shown in Table 1, after the introduction of electric springs for optimization, the total operating cost, power purchase cost, storage charging and discharging cost and reliability cost are all reduced, and some customers of CLs are willing to pay part of their electricity bills more because of the high reliability guarantee due to the introduction of electric springs, thus increasing the total electricity benefit on the operator's side. As a result, although the microgrid operator has to pay some additional ES usage and depreciation costs, the economic benefits and voltage stability of the whole distribution network are significantly improved.

After adding ES, ES regulates NLs to increase active power consumption during wind power affluence and storage charging, which reduces the storage charging power and increases wind power consumption in some periods. Further analysis is easy to obtain that with the rated power of NLs, ES can regulate their power consumption upward or downward, thus reducing the microgrid's power demand for DG and energy storage, and even the climbing capacity demand.

Especially for energy storage, ES moderated charging and discharging power is equivalent to adding a part of virtual capacity for energy storage, thus making the economy of microgrid operators and NL users improved. In addition, after the NL is retrofitted with ES to form a power consumption group with the CL, the voltage deviation rate and fluctuation rate are significantly improved, and the high reliability power demand of the CL users is guaranteed.

5.3. Simulation Analysis of Multi-Scene Energy Optimization

Since the microgrid energy optimization scheme containing ES is affected by the inputs of distributed power supply (all to this) output, load demand and day-ahead tariff, in order to verify the effectiveness of this optimization scheme under different input conditions, eight typical scenarios are formed according to the combination of distributed power supply output size, NL power factor and day-ahead market tariff (large distributed power supply output corresponds to scenario 1 4, small wind power output corresponds to scenarios 5-8; high NL power factor corresponds to scenarios 1, 2, 5 and 6, low NL power factor corresponds to scenarios 3, 4, 7 and 8; high day-ahead tariff corresponds to scenarios 1, 3, 5 and 7, low day-ahead tariff corresponds to scenarios 2 and 8 or comparison, as shown in Table 2.

**Table 2.** Comparison of various costs before and after optimization

Scene No.	Distributed power out	NL power factor	Current market tariff
1	Big	High	High
2	Big	High	Low
3	Big	Low	High
4	Big	Low	Low
5	small	High	High
6	small	High	Low
7	small	Low	High
8	small	Low	Low

In this section, based on the above scenarios 1-8 and randomly generating the probability of occurrence of each scenario, we analyze the impact of uncertainties of distributed power output size, load weight and day-ahead tariff on the microgrid energy optimization model. The probabilities of scenarios 1-8 are 0.1, 0.2, 0.05, 0.15, 0.2, 0.15, 0.05, and 0.1, respectively, and the simulation results including economic cost and voltage deviation are obtained according to the optimization objectives of accounting for uncertainty shown in Eq. (21), as shown in Table 3.

**Table 3.** Comparison of various costs before and after optimization

Indicators	Before optimization	After optimization	Amount of change
------------	---------------------	--------------------	------------------

Total operating cost /yuan	6261.86	6047.93	-213.93
Base operating cost of microgrid /yuan	6261.86	6011.47	-250.39
Additional costs associated with electric springs /yuan	0	36.46	35.29
Power purchase cost /yuan	3569.90	3535.57	-34.33
Energy storage charging and discharging cost /yuan	1443.7	1270.1	-173.6
Reliability cost/yuan	768.65	694.03	-74.62
Wind abandonment cost /yuan	1081.2	1046.3	-34.9
Cost of light abandonment /yuan	953.3/\$	928.2	-25.1
Average voltage deviation/%	2.75	2.68	-0.07

The energy optimization model considering 8 scenarios and 3 uncertainty factors is equivalent to a comprehensive optimization model that evaluates multiple scenarios in general, and the conclusions obtained are related to the probability of occurrence of each scenario. The mathematical nature of the comprehensive optimization model is more complex compared with the single optimization model, so the conclusions reached have a certain evaluation significance, and when evaluating the pros and cons of ES applications using the multi-scenario energy optimization model proposed in this paper The conclusions obtained are therefore of a certain evaluative significance when evaluating the advantages and disadvantages of ES applications using the multi-scenario energy optimization model proposed in this paper.

The conclusion reached with the optimization objective of maximizing the expected revenue of the microgrid operator is basically the same as that of the eight scenarios optimized individually above. That is, at this time in ES can regulate the NL so as to balance the distribution network load, consume distributed energy and play a certain virtual energy storage effect, thus reducing the cost of power purchase, storage charging and discharging costs, improving the distribution network reliability, stabilizing the node voltage and reducing the waste of distributed energy such as wind and light.

It is worth noting that in different scenarios, the addition of ES also increases part of the total microgrid cost, such as the maintenance cost of ES; at the same time, the regulation of the ES makes some Intelligent load users suffer some loss of benefits and thus need to be compensated, thereby leading to a slight increase in the optimized Intelligent load electricity expenditure in some cases, which is due to the sub-scenarios within the integrated optimization model. The optimization

results of the variables optimized individually are different, and the expected value of the increased electricity expenditure of Intelligent load exceeds the expected value of the regulation subsidy, when other measures need to be considered to continue to maintain the willingness of NL users to install ES.

The above simulation analysis shows that ES can reduce wind and light abandonment by regulating the power consumption of NLs and reduce the storage charging and discharging power, which can basically achieve a win-win situation for the economic benefits of operators and Intelligent load users. The Intelligent load sacrifices its own voltage quality to improve the reliability of power supply for CLs, which has certain practical significance and application value in the microgrid where the scenery access rate is high and the voltage quality needs to be improved. The high reliable power supply guarantee fee for CLs mainly leads to a small increase in the total load tariff without affecting the normal electricity consumption of other common loads.

## 6. Conclusion

In this paper, we propose a microgrid source-load-storage cooperative dispatching model with ES, and we optimize the source-load-storage cooperative dispatching for microgrid with the objectives of maximum economic benefits for microgrid operators and optimal voltage level of microgrid nodes, in which the role of ES as a NL regulating medium is reflected in both reducing the charging and discharging power of energy storage system and increasing the local consumption of renewable energy, which basically achieves a win-win situation for operators and The multi-win situation of operators and multiple load users is basically realized. And the optimal scheduling scheme of this model is obtained by quantum particle swarm algorithm with improved chaotic mapping. Finally, the scheduling of a region in Tianjin within 24h is used as a case study to compare the simulation results before and after optimization, and the correctness and feasibility of the model proposed in this paper are verified, and the following conclusions can be obtained:

(1) In the optimal dispatching scheme after the introduction of ES for dispatching, the total operating cost of the microgrid is reduced and the node voltage deviation situation is significantly improved, which indicates that the addition of ES can help the microgrid achieve low-cost and stable operation.

(2) The introduction of ES not only realizes the balance between NL and CL, but also helps coordinate conventional energy and DG, improves the utilization rate of DG and realizes source-load complementarity; in addition, the introduction of ES somehow realizes the effect of virtual energy storage and reduces the cost of energy storage charging and discharging, thus truly realizing the cooperative dispatch of source-load storage.

(3) In several scenarios with different DG output, different power factors of NLs, and different day-ahead tariffs, ES can achieve the effect of reducing operating costs and balancing node voltages, which indicates the wide application of ES in microgrid dispatching.

The proposed model and simulation conclusions can provide ideas for the application of ES in microgrids, and provide references for microgrid operators with high proportion of distributed power supply access to expand profitability and improve the quality of power supply services. The next research direction is to quantitatively analyze in which microgrid operation scenarios ES does not bring economic improvement, and to study the applicability of the proposed optimization model in practical conditions and the application mode of ES in a more detailed and extensive way.

**Appendix A**

**Table A1.** Parameters of microgrid

Parameter Name	Parameter values (Unit)
installed capacity of wind power	1.8 (MW)
peak load of wind power	1.2 (MW)
installed capacity of photovoltaic power	1.8 (MW)
peak load of photovoltaic power	1.2 (MW)
unit price of gas turbine power generation	0.52 (yuan/(kW·h))
cost of abandoned wind and light	0.8 (yuan/(kW·h))

**Table A2.** Parameters of energy storage equipment

Parameter Name	Parameter values (Unit)
Charging power limit	800 (kW)
Discharge power limit	600 (kW)
Upper limit of charge state	90 (%)
Lower limit of charge state	20 (%)
Self-discharge rate of energy storage	0.001 (%)
Energy storage and discharge efficiency	92 (%)
Energy storage charging efficiency	92 (%)
Battery life cycle	3.0 (year)
Interest Rate	6.5 (%)
Annuity Factor	0.2406
Investment cost factor	1.9

**Table A3.** Parameters of Load

Parameter Name	Parameter values (Unit)
Unit regulation compensation for interruptible loads	0.8 (kW·h)
Unit regulation allowance for smart loads	0.4 (kW·h)
High reliability coverage paid extra for CLs	0.02 (kW·h)
The upper limit of the intelligent load acceptance regulation	5 (%)
The lower limit of the intelligent load acceptance regulation	10 (%)

**Acknowledgements**

This paper was supported by the Science and Technology Project of State Grid Shandong Electric Power Company (Granted No. 520604230004).

**References**

[1] C. Yin, N. Quan, K. Su, Z. Zheng, T. Zhang. "Status and Outlook of Distributed Energy Development in China." *Distributed Energy*, vol. 2, pp. 1-7, July 2022.

[2] Z. Zhang, Y. Zhang, Q. Huang, W. Lee. "Market-oriented optimal dispatching strategy for a wind farm with a multiple stage hybrid energy storage system." *CSEE Journal of Power and Energy Systems*, vol. 4, pp.417-424, April 2018.

[3] H. Ding, P. Pinson, Z. Hu, Y. Song,. "Integrated bidding and operating strategies for wind-storage systems." *IEEE Transactions on Sustainable Energy*, vol. 1, pp.163-172, July 2016.

[4] N. Zhang, N. C. Yang, J. H. Liu. "Optimal Time-of-Use Electricity Price for a Microgrid System Considering Profit of Power Company and Demand Users." *Energies*, vol. 14, pp.6333-6345, July 2021

[5] M. Mishel, S. Pourya, B. Fahimi. "Economic Dispatch of a Hybrid Microgrid With Distributed Energy Storage." *IEEE Transactions on Smart Grid* “, vol. 6, pp. 2607-2614, June 2015.

[6] Z. Zhang, Z. Wang, R. Cao, H. Zhang. "Research on Two-Level Energy Optimized Dispatching Strategy of Microgrid Cluster Based on IPSO Algorithm." *IEEE Access*, vol. 9, pp. 2169-3536, September 2021.

[7] J. Han, L. Yan, Z.A. Li. "A Multi-Timescale Two-Stage Robust Grid-Friendly Dispatch Model for Microgrid Operation." *IEEE Access*, vol. 8, pp. 74267-74279, August 2020.

- [8] R. Huisy, K. Leec, F. Wu. "Electric springs-A new smart grid technology." *IEEE Transactions on Smart Grid*, vol. 3, pp. 1552-1561, March 2012.
- [9] S. Yan, C. Lee, T. Yang, K. Mok, S. Tan. "Extending the Operating Range of Electric Spring Using Back-To-Back Converter: Hardware Implementation and Control." *IEEE Transactions on Power Electronics*, 2017(7):5171-5179.
- [10] Z. Ren, M. Pham, T. Song, D. Kim. "A Robust Global Optimization Algorithm of Electromagnetic Devices Utilizing Gradient Index and Multi-Objective Optimization Method." *IEEE Transactions on Magnetism*, vol. 47, pp.1254-1257, May 2011.
- [11] E. Reid, S. Vander, A. Danie, D.M. Abraham. "Multi-Objective Optimization Models for Improved Decision-Support in Humanitarian Infrastructure Project Selection Problems." *IEEE Systems Journal*, vol. 2, pp. 536-547, April 2008.
- [12] X. Chen, Y. Hou, S. Tan, C. Lee, S. Hui. "Mitigating Voltage and Frequency Fluctuation in Microgrids Using Electric Springs." *IEEE Transactions on Smart Grid*, vol. 6, pp. 508-515, June 2015.
- [13] Y. Zhang, G. Yang, G. Zhang. "A survey of alternating current electric spring topologies: from the view of the topology functions." *Control Theory & Applications*, vol. 36, pp.1369-1381, September 2019.
- [14] C. Wang, S. Mei, H. Yu, S. Cheng, L. Du, P. Yang. "Unintentional Islanding Transition Control Strategy for Three-/Single-Phase Multimicrogrids Based on Artificial Emotional Reinforcement Learning." *IEEE Syst. J.*, vol. 15, pp. 5464-5475, 2021.
- [15] B. Keqin, W. Haoqiang, C. Qiming, C. Haiyan. "Passive control strategy of electric spring based on E-L model." *High Volt. Technol*, vol. 10, pp. 1-10, October 2021.
- [16] L. Liang, Y. Hou, J. Hill, S.Y.R. Hui. "Enhancing resilience of microgrids with electric spring." *IEEE Trans. Smart Grid*, vol. 9, pp. 2235-2247, September 2018.
- [17] B. W. Dong, H. Xue, Y.J. Hu. "Voltage Stabilization Control Method of Renewable Energy Power Supply System Based on Electric Spring." *Electr. Meas. Instrum*, vol. 57, pp.100-107, December 2020.
- [18] H. Shahinzadeh, J. Moradi, W. Yaïci, M. Longo and Z. Azani, "Impacts of Energy Storage Facilities on Resilient Operation of Multi-Carrier Energy Hub Systems," *International Conference on Smart Grid (icSmartGrid)*, IEEE, vol. 10, pp. 339-344, June 2022.
- [19] T. Yang, K.T. Mok, S.S. Ho, S.C. Tan, C.K. Lee, R.S. Hui. "Use of integrated photovoltaic-electric spring system as a power balancer in power distribution networks." *IEEE Trans. Power Electron*, vol. 34, pp.5312-5324, December 2019.
- [20] M. Wang, S. Yan, S. Tan, S. Hui. "Hybrid-DC electric springs for DC voltage regulation and harmonic cancellation in DC microgrids." *IEEE Trans. Power Electron*, vol. 33, pp.1167-1177, November 2018.
- [21] J. Soni, B. Sen, V.K. Kanakesh, S.K. Panda. "Performance analysis and evaluation of reactive power compensating electric spring with linear loads." *International Journal of Electrical Power & Energy Systems*, 2018(101), 116-126.
- [22] Z. Wang, S. Yan, Y. Tang, X. Men, J. Cao. "Low carbon economy operation and energy efficiency analysis of integrated energy systems considering LCA energy chain and carbon trading mechanism." *Proceedings of the CSEE*, vol. 39, pp.1614-1626, June 2019.
- [23] Z. Zhao, M. Liu. "Energy Sharing Model of Virtual Power Plant Considering the Lifetime Cost of Energy Storage." *Distributed Energy*, vol. 7, pp. 21-29, June 2022.
- [24] N. Liu, L. Tan, H. Sun, Z. Zhou, B. Guo. "Bilevel heat-electricity energy sharing for integrated energy systems with energy hubs and prosumers." *IEEE Trans. Ind. Informatics*, vol. 18, pp. 3754-3765, June 2022.
- [25] Y. Huang, Q. Zhang, M. Kang. "Energy scheduling framework of micro-grids considering battery lifetime." *IEEE Access*, vol. 10, pp. 25016-25024, 2022.
- [26] H. Shahinzadeh, S. Nikolovski, J. Moradi and R. Bayindir, "A Resilience-Oriented Decision-Making Model for the Operation of Smart Microgrids Subject to Techno-Economic and Security Objectives," *International Conference on Smart Grid (icSmartGrid)*, IEEE, vol. 9, pp. 226-230, June 2021.
- [27] Z. Wang, C. Qiao, T. Liu, Z. Li, X. Liu, R. Zhao, K. Wan. "Optimization of the CCHP System Operation Strategy Under the Background of Carbon Peaking and Carbon Neutrality." *Distributed Energy*, vol. 7, pp. 17-22, May 2022.
- [28] B. Jin, H. Ahmadi, A. Behbahani, F. Torabi. "Techno-Economic Analysis of Deep Peak Regulation of Combined Heat and Power Units Considering the Benefits of Auxiliary Service." *Distributed Energy*, vol. 7, pp. 52-59, June 2022.
- [29] G. He, L. Lu. "An improved QPSO algorithm and its application in fuzzy portfolio model with constraints." *Soft Computing*, vol. 25, pp. 7695-7706, June 2021.
- [30] M. Garba, M. A. Tankari and G. Lefebvre, "Using of distributed energy resources for microgrid resilience achieving," *International Conference on Renewable Energy Research and Applications (ICRERA)*, IEEE, vol. 6, pp. 659-663, November 2017.